

Generation of 206.8 nm GHz deep-ultraviolet femtosecond pulses via cascaded fifth-harmonic generation from a Kerr-lens mode-locked Yb:$CaYAlO_4$ oscillator

Dongyang Zou(邹东阳), Mojun Pan(潘默君), Runze Wang(王润泽), Runji Li(李润基), Li Zheng(郑立), Jiangfeng Zhu(朱江峰), Chenxia Yun(运晨霞), Baiqing Lv(吕佰晴), Hong Ding(丁洪)
Citation: Chin. Phys. B. 35, 094210 (2026). DOI: 10.1088/1674-1056/ae8002 |
CSTR: 32038.14.CPB.ae8002
http://cpb.iphy.ac.cn; http://iopscience.iop.org/cpb

What follows is a list of articles you may be interested in

Generation ofWatt-level Kerr-lens mode-locked Yb:CYA laser at 1-GHz repetition rate

Guodong Zhao(赵国栋), Junyi Ma(马骏逸), Hainian Han(韩海年), Zhaohua Wang(王兆华), Zhiyi Wei(魏志义)
Chin. Phys. B. 34, 084204 (2025). DOI: 10.1088/1674-1056/adcf8b | CSTR: 32038.14.CPB.adcf8b

Numerical study of converting beat-note signals of dual-frequency lasers to optical frequency combs by optical injection locking of semiconductor lasers

Chenhao Liu(刘晨浩), Haoshu Jin(靳昊澍), Hui Liu(刘辉), Jintao Bai(白晋涛)
Chin. Phys. B. 31, 084205 (2022). DOI: 10.1088/1674-1056/ac649a

Optomechanical-organized multipulse dynamics in ultrafast fiber laser

Lin Huang(黄琳), Yu-Sheng Zhang(张裕生), Yu-Dong Cui(崔玉栋)
Chin. Phys. B. 30, 114203 (2021). DOI: 10.1088/1674-1056/abf344

Mid-infrared supercontinuum and optical frequency comb generations in a multimode tellurite photonic crystal fiber

Xu Han(韩旭), Ying Han(韩颖), Chao Mei(梅超), Jing-Zhao Guan(管景昭), Yan Wang(王彦), Lin Gong(龚琳), Jin-Hui Yuan(苑金辉), Chong-Xiu Yu(余重秀)
Chin. Phys. B. 30, 094207 (2021). DOI: 10.1088/1674-1056/abf10f

High power diode-pumped passively mode-locked Nd:YVO4 laser at repetition rate of 3.2 GHz

Meng-Yao Cheng(程梦尧), Zhao-Hua Wang(王兆华), Yan-Fang Cao(曹艳芳), Xiang-Hao Meng(孟祥昊), Jiang-Feng Zhu(朱江峰), Jun-Li Wang(王军利), Zhi-Yi Wei(魏志义)
Chin. Phys. B. 28, 054205 (2019). DOI: 10.1088/1674-1056/28/5/054205

RAPID COMMUNICATION

Generation of 206.8 nm GHz deep-ultraviolet femtosecond pulses via cascaded fifth-harmonic generation from a Kerr-lens mode-locked Yb:$CaYAlO_4$ oscillator

Dongyang Zou(邹东阳)[1,2,†], Mojun Pan(潘默君)[1,3,†], Runze Wang(王润泽)[1], Runji Li(李润基)[1], Li Zheng(郑立)[4], Jiangfeng Zhu(朱江峰)[5], Chenxia Yun(运晨霞)[6], Baiqing Lv(吕佰晴)[1,3,7,‡], and Hong Ding(丁洪)[1,2,8]

[1] *Tsung-Dao Lee Institute & School of Physics and Astronomy, Shanghai Jiao Tong University, Shanghai* 200240, *China*
[2] *Hefei National Laboratory, Hefei* 230088, *China*
[3] *Shanghai Research Center for Quantum Sciences, Shanghai* 201315, *China*
[4] *School of Physics and Telecommunication Engineering, Shaanxi University of Technology, Hanzhong* 723001, *China*
[5] *School of Optoelectronic Engineering, Xidian University, Xi'an* 710071, *China*
[6] *Beijing National Laboratory for Condensed Matter Physics and Institute of Physics, Chinese Academy of Sciences, Beijing* 100190, *China*
[7] *Zhangjiang Institute for Advanced Study, Shanghai Jiao Tong University, Shanghai* 200240, *China*
[8] *New Cornerstone Science Laboratory, Tsung-Dao Lee Institute, Shanghai Jiao Tong University, Shanghai* 200240, *China*

(Received 9 May 2026; revised manuscript received 16 June 2026; accepted manuscript online 22 June 2026)

We report the generation of 206.8 nm deep-ultraviolet (DUV) femtosecond pulses with an average power of 10.2 mW at a repetition rate of 1.08 GHz. The DUV radiation is obtained via cascaded fifth-harmonic generation (FiHG) directly driven by a Kerr-lens mode-locked (KLM) Yb:$CaYAlO_4$ (Yb:CYA) oscillator, employing lithium triborate (LBO) and β-barium borate (BBO) crystals for successive second-, third-, and fifth-harmonic conversion. Maximum average powers of 2.32 W at 518.9 nm and 1.23 W at 345.2 nm are achieved, corresponding to conversion efficiencies of 33.7% and 18.6%, respectively, while 10.2 mW is obtained at 206.8 nm with an overall efficiency of 0.148%. By intentionally employing thick nonlinear crystals to reduce the phase-matching bandwidth, a narrow energy resolution of 2.75 meV is achieved. This is the first demonstration of direct FiHG to 206.8 nm driven by a GHz femtosecond oscillator. This approach provides a practical route toward compact DUV sources that simultaneously combine GHz repetition rate and meV-level energy resolution for high-resolution ARPES.

Keywords: DUV femtosecond pulses, GHz repetition rate, narrow energy resolution, angle-resolved photoemission spectroscopy (ARPES)

PACS: 42.65.Ky, 79.60.–i, 79.60.–i

DOI: 10.1088/1674-1056/ae8002 **CSTR:** 32038.14.CPB.ae8002

1. Introduction

DUV femtosecond lasers generated via high-order harmonic conversion provide unique advantages due to their short wavelength and high photon energy, enabling high spatial resolution, reduced diffraction, and cold material processing.[1–3] These features have enabled broad applications in precision manufacturing, spectroscopy, and biomedicine.[4–7] In particular, photons with energies around 6 eV are well suited for probing electronic structures and molecular bonds, making DUV sources highly relevant for photoemission and imaging applications.[8]

In addition to wavelength scaling, repetition rate plays a critical role in practical performance. Compared with conventional kHz–MHz systems, GHz-repetition-rate lasers significantly improve processing efficiency, reduce thermal damage, and enhance temporal resolution in ultrafast spectroscopy.[9–12] In ARPES, GHz sources are especially advantageous, as they suppress space-charge effects and enable rapid data acquisition, which is essential for studying fragile quantum materials with limited surface lifetimes.[13,14]

Despite these advantages, realizing short-wavelength DUV radiation at GHz repetition rates remains challenging. Conventional sources, such as fourth-harmonic generation by excimer lasers and Ti:sapphire lasers, are limited by low repetition rates, poor beam quality, or low conversion efficiency.[15–18] Yb-based oscillators provide a promising route toward GHz operation; however, their low pulse energy (nJ–pJ level) makes high-order nonlinear conversion highly inefficient, particularly for FiHG in the DUV region.[19,20] Furthermore, most ultrafast DUV sources prioritize short pulse duration, resulting in broad spectral bandwidth that limits their applicability in high-resolution ARPES. Achieving both high

[†] These authors contributed equally to this work.
[‡] Corresponding author. E-mail: baiqing@sjtu.edu.cn
© 2026 Chinese Physical Society and IOP Publishing Ltd. All rights, including for text and data mining, AI training, and similar technologies, are reserved.

repetition rate and narrow energy bandwidth therefore remains an open challenge.[21]

Here, we address these challenges by combining GHz femtosecond operation with phase-matching bandwidth engineering. We demonstrate, for the first time, direct FiHG to 206.8 nm (6 eV) from a GHz Kerr-lens mode-locked Yb oscillator.[22] By intentionally employing thick nonlinear crystals to suppress the phase-matching bandwidth, we achieve meV-level energy resolution in the DUV output. This work bridges the gap between short-wavelength DUV generation and GHz repetition-rate operation, providing a compact and practical light source for high-resolution ARPES.

2. Experimental setup

Figure 1 shows the experimental setup for generating the 206.8 nm DUV laser. The system consists of three cascaded frequency-conversion stages — second-, third-, and fifth-harmonic generation (SHG, THG, and FiHG) — all driven by a homemade GHz Kerr-lens mode-locked Yb:CYA oscillator. The fundamental source delivers 121.5 fs pulses with 8.34 W average power at a repetition rate of 1.08 GHz, centered at 1037 nm with a full width at half maximum (FWHM) of 10.9 nm.[23]

The fifth harmonic (5ω) is generated using a cascaded "$2+3$" sum-frequency scheme. The second harmonic (2ω) is first produced via SHG and then mixed with the fundamental (ω) to generate the third harmonic (3ω) through THG. Subsequently, the 2ω and 3ω beams are combined to generate the 5ω output. To achieve narrow spectral bandwidth, relatively thick nonlinear crystals are deliberately employed in all conversion stages to reduce the phase-matching bandwidth, enabling high energy resolution in the DUV output.

As shown in Fig. 1, the fundamental beam is focused into a 5-mm-thick LBO ($\theta = 0°$, $\phi = 13.5°$) crystal for SHG, and the generated 2ω beam is separated by dichroic mirrors, collimated, and polarization-adjusted before being recombined with the fundamental beam for THG in a 5-mm-thick BBO ($\theta = 32.5°$) crystal. Temporal synchronization between the ω and 2ω pulses is achieved using a quartz delay window inserted in the 2ω path. For FiHG, the 3ω beam is separated from the lower harmonics, while the 2ω beam is redirected and recombined with the 3ω beam. Both beams are collimated and focused into a 7-mm-thick BBO ($\theta = 77.3°$) crystal for sum-frequency generation to 206.8 nm. The generated 5ω beam is finally separated from the residual beams using a pair of fused silica prisms.

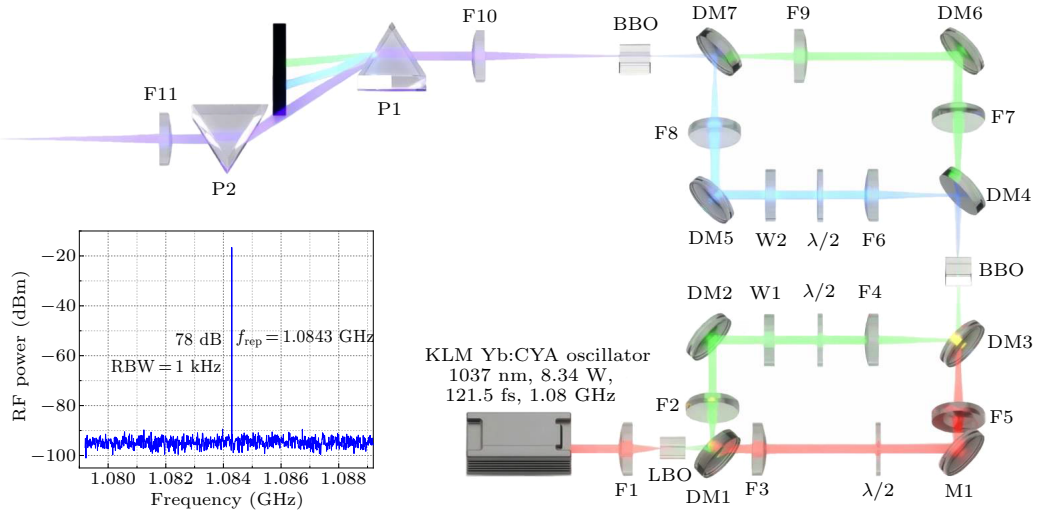


Fig. 1. The schematic diagram of the experimental setup for generating the 206.8 nm laser, consisting of three cascaded stages: SHG, THG and FiHG. ($\lambda/2$, half wave plate; TFP, thin-film polarizer; F1–F9, plane-convex lens; M, mirror; DM, dichroic mirror; W, window; P, silica equilateral prisms. M1, HR coated at 1030 nm; DM1&DM2&DM3&DM6, HR coated at 515 nm and AR coated at 1030 nm; DM4&DM5&DM7, HR coated at 343 nm and AR coated at 1030 nm & 515 nm.) The inset shows the repetition rate of the fundamental laser.

3. Experimental results

This section summarizes the performance of the cascaded frequency conversion processes, including SHG, THG, and FiHG.

Figure 2(a) shows the spectrum of the SHG output centered at 518.9 nm with a FWHM of 2.65 nm, corresponding to a Fourier-transform-limited pulse duration of 107 fs (assuming a sech^2 profile). The inset of Fig. 2(a) shows that the measured pulse duration is 156 fs (APE PulseCheck USB).

Figure 2(b) presents the THG spectrum centered at 345.2 nm with a FWHM of 0.85 nm. As shown in Fig. 2(c), an SHG output power of 2.32 W is obtained at a fundamental power of 6.88 W, corresponding to a conversion efficiency of 33.7%. The efficiency is not saturated due to the relatively limited peak intensity (18.2 GW/cm^2) of the GHz source, and can be further improved with higher input power. Tian *et al.* reported that a conversion efficiency of 59% was achieved for SHG at 37 GW/cm^2 pump intensity based on a MHz-repetition-rate oscillator with a pulse duration of 153 fs.[24] As shown in

Fig. 2(d), an output power of 1.23 W at 345.2 nm is achieved under a 6.61 W fundamental pump, corresponding to an overall conversion efficiency of 18.6% from 1037 nm. Figure 2(e) shows the 100-min free-running power fluctuation of the SHG output, with an RMS of 0.219% at 2.32 W. The THG output exhibits an RMS fluctuation of 0.588% at 1.196 W over the same duration [Fig. 2(f)], indicating excellent operational stability.

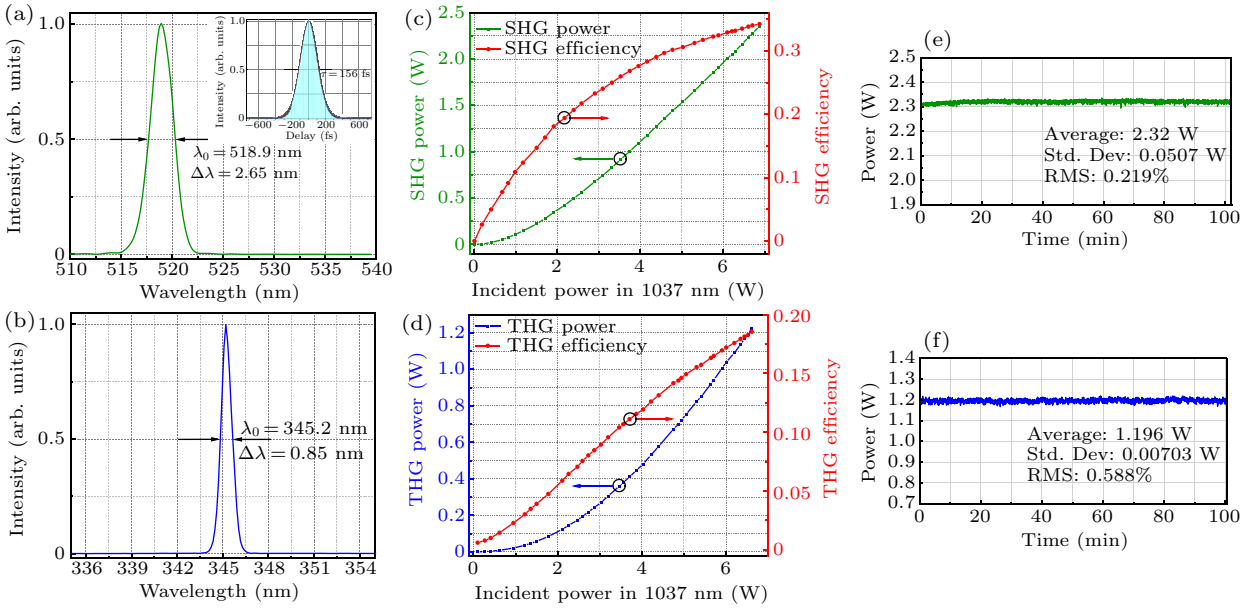


Fig. 2. Characterization of SHG and THG. (a) The spectrum and pulse duration of SHG. (b) The spectrum of THG. (c), (d) Output powers and corresponding conversion efficiencies of SHG and THG versus fundamental power. (e), (f) Power stability of SHG and THG over 100 min.

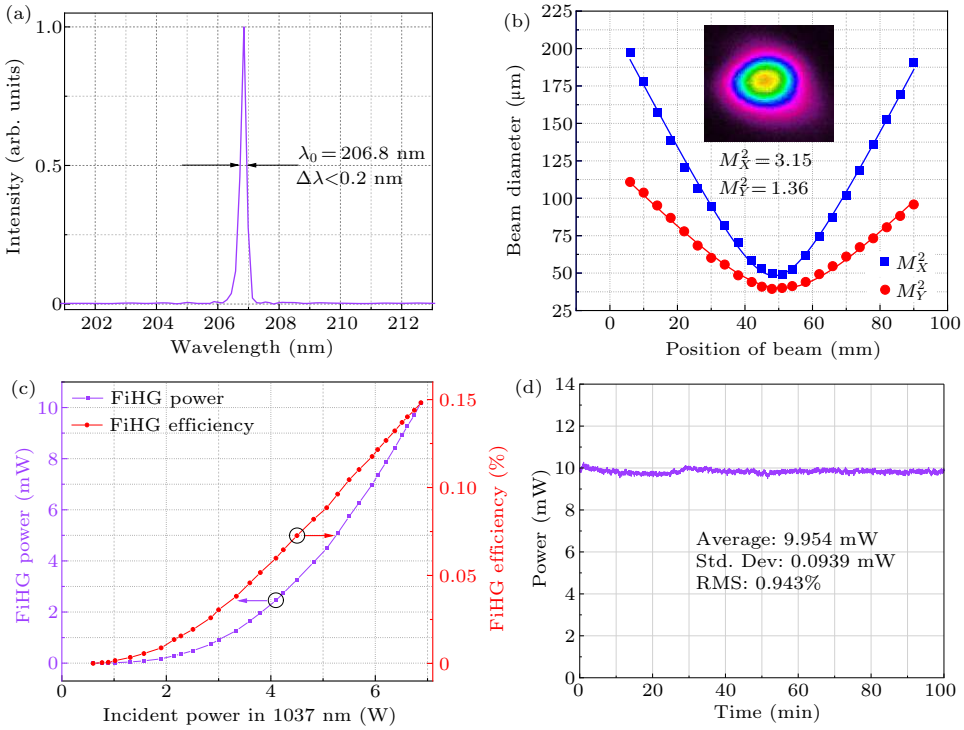


Fig. 3. Characterization of FiHG. (a) The spectrum of FiHG. (b) Beam quality and near-field beam spot. (c) Output power and corresponding conversion efficiency versus fundamental power. (d) Power stability over 100 min.

The FiHG spectrum is shown in Fig. 3(a), centered at 206.8 nm. Due to the limited resolution of the spectrometer, the spectral bandwidth is characterized via ARPES measurements. Figure 3(b) presents the beam quality of the 206.8 nm output, with M^2 values of 3.15 and 1.36 along the horizontal and vertical directions, respectively. This anisotropy arises from birefringent walk-off in the BBO crystal, which becomes more pronounced with increasing crystal thickness. While thicker crystals effectively reduce the phase-matching bandwidth, they also degrade beam quality due to accumulated spa-

tial walk-off. At a fundamental power of 6.87 W, an output power of 10.2 mW is obtained at 206.8 nm, corresponding to an overall conversion efficiency of 0.148% [Fig. 3(c)]. The long-term stability is shown in Fig. 3(d), with an RMS fluctuation of 0.943% over 100 min at 9.95 mW.

The instrumental energy resolution is determined from the energy distribution curve (EDC) acquired at the Fermi edge of a polycrystalline gold sample measured at 10 K. By fitting this single EDC trace with a convolution of a Gaussian function and the Fermi–Dirac distribution, an energy resolution of 2.75 meV is obtained, corresponding to a spectral bandwidth of 0.095 nm. For further improvement of the energy resolution, one can incorporate a narrowband filter into the fundamental beam path to narrow its spectral linewidth, or adopt type-II phase matching in the THG process to achieve a narrower phase-matching bandwidth. The above approaches will lead to reduced conversion efficiency and exacerbated beam walk-off effect, respectively, which require comprehensive consideration in practical implementation. Figure 4(b) shows ARPES measurements of Bi_2Se_3 at the Γ point at 10 K, demonstrating excellent energy and angular resolution. The Fermi level surface is presented in the inset of Fig. 4(b).

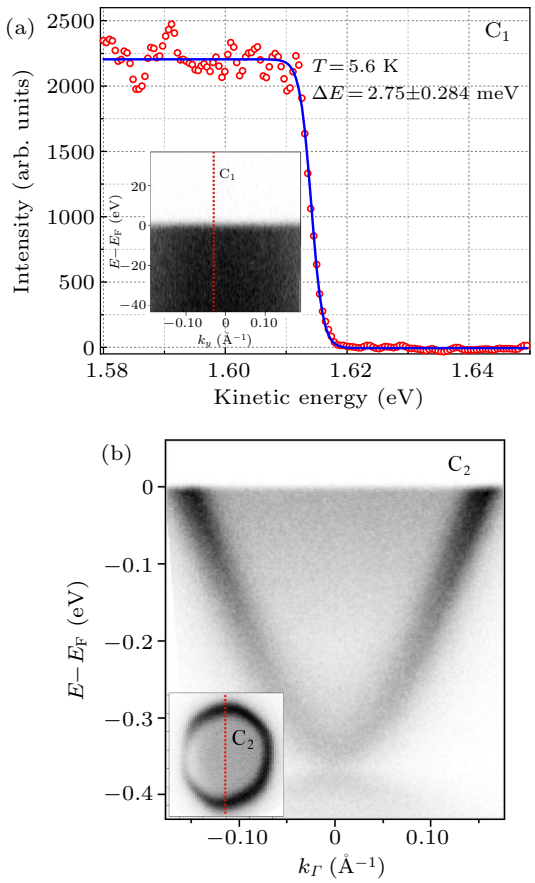


Fig. 4. Performance of the 6 eV laser in the ARPES measurements. (a) EDC measured at the Fermi edge of polycrystalline gold, with the corresponding fitting curve for energy resolution calibration. (b) Band structure of Bi_2Se_3 at the Γ point measured by 6 eV laser.

4. Conclusion

In conclusion, we have demonstrated 206.8 nm DUV femtosecond pulses at a repetition rate of 1.08 GHz via direct fifth-harmonic generation from a Kerr-lens mode-locked Yb:CYA oscillator. By employing thick nonlinear crystals to engineer the phase-matching bandwidth, a narrow energy resolution of 2.75 meV is achieved. This work establishes a practical approach to simultaneously realize GHz repetition rate and meV-level energy resolution in DUV sources. The demonstrated system is particularly attractive for ARPES, where high repetition rate suppresses space-charge effects while narrow bandwidth enables high-resolution measurements. Our results highlight the importance of bandwidth engineering in ultrafast nonlinear optics and provide a scalable route toward compact, high-performance DUV light sources for quantum materials research.

Acknowledgements

B. L. acknowledges support from the National Key R&D Program of China (Grant No. 2023YFA1407400), the National Natural Science Foundation of China (Grant No. 12374063), the Shanghai Natural Science Fund for Original Exploration Program (Grant No. 23ZR1479900), and the Cultivation Project of Shanghai Research Center for Quantum Sciences (Grant No. LZPY2024). H. D. acknowledges support from the Innovation Program for Quantum Science and Technology (Grant No. 2021ZD0302700), the New Cornerstone Science Foundation (Grant No. 23H010801236), and the National Natural Science Foundation of China (Grant No. 12488101). L. Z. acknowledges support from the National Natural Science Foundation of China (Grant No. 62405171)

References

[1] Delmdahl R, Paetzel R 2010 *ICALEO* **103** 1323
[2] Zhu X N and Bao W X 2019 *Chin. J. Lasers* **46** 1200001
[3] Cui Z Q and Guan Y C 2020 *Laser Optoelectron. Prog.* **57** 14
[4] Shi Y Q, Cui Z J, Sun M Y, Guo Y J, Xu J Z, Xie X L, Liu D A and Zhu J Q 2025 *Opt. Lett.* **50** 1136
[5] Quito C F G, Agahan A L D and Evangelista R P 2013 *Int. Sch. Res. Notices* **2013** 276984
[6] Belli F, Kotsina N, Gao S F, Wang Y Y, Wang P, John C T and Townsend D 2019 *CLEO/Europe-EQEC* ee_5_1
[7] Teles-Ferreira D C, Manzoni C, Martínez-Fernández L, Cerullo G, de Paula A M and Borrego-Varillas R 2022 *Molecules* **27** 041200
[8] Jennifer S B, Lindsay J M and Santos I C 2019 *Chem. Rev.* **120** 3328
[9] Kerse C, Kalaycioglu H, Elahi P, Cetin B, Kesim D K, Akcaalan O, Yavas S, Asik M D, Oktem B and Hoogland H 2016 *Nature* **537** 84
[10] Li Q M, Bai H Z, Teng X D, Chen H S, Mai H J, Zhang Z T, Zhang J W and Xuan H W 2025 *Ultrafast Sci.* **5** 0087
[11] Pinkowski N, Ding Y M, Strand C, Hanson R, Horvath R and Geiser M 2020 *Meas. Sci. Technol.* **31** 055501
[12] Ji N, Magee J and Betzig E 2008 *Nat. Methods* **5** 197
[13] Belloni V, Pinaud M, Delahaye H, Furfaro L, Pontagnier L, Santarelli G, Cormier E, Froehly L and Courvoisier F 2025 *Opt. Express* **33** 26139
[14] Zhou X J, He S L, Liu G D, Zhao L, Yu L and Zhang W T 2018 *Rep. Prog. Phys.* **81** 062101

[15] Tanaka S, Arakawa M, Fuchimukai A, Sasaki Y, Onose T, Kamba Y, Igarashi H, Qu C, Tamiya M and Oizumi H 2016 *Proc. SPIE* **9726** 972624
[16] Chen C T, Lu J H, Togashi T, Suganuma T, Sekikawa T, Watanabe S, Xu Z Y and Wang J Y 2002 *Opt. Lett.* **27** 637
[17] Yoshino K, Hayashi S and Sugimoto R 1984 *JJAP* **23** L899
[18] Eichner T, Jiang M, Gonzalez-Diaz J, Hülsenbusch T, Braun C, Thesinga J, Werle C, Winkelmann L, Yousefi A, Pergament M, Leemans W, Maier A and Palmer G 2025 *Opt. Lett.* **50** 4890
[19] Zhang Z Y, Ma J Y, Zhao G D, Shao X D, Zheng Y Z, Han H N and Wei Z Y 2023 *Front. Phys.* **11** 1116054
[20] Zhao G D, Ma J Y, Han H N, Wang Z H and Wei Z Y 2025 *Chin. Phys. B* **34** 084204
[21] Zheng J Q, Cong Z H, Liu Z J, Wang S and Zhao Z G 2021 *Chin. J. Lasers* **48** 1201008
[22] Guo Q D, Dendzik M, Grubišić-Čabo A, Berntsen M H, Li C, Chen W Y, Matta B, Starke U, Hessmo B, Weissenrieder J and Tjernberg O 2022 *Struct. Dyn.* **9** 024304
[23] Zheng L, Bai J X, Wang G Y, Tian W L, Wei Z Y and Zhu J F 2025 *Opt. Lett.* **50** 4998
[24] Tian W L, Tian X, Li Q, Wang G Y, Bai C, Yu Y, Xu X D, Xu J, Wei Z Y and Zhu J F 2023 *Opt. Lett.* **48** 4789